

## 表面强化及功能化

材料表面微纳形貌对血管细胞  
行为影响的研究综述

李昱彤, 裴佳, 袁广银

(上海交通大学 材料科学与工程学院 轻合金精密成型国家工程研究中心  
金属基复合材料国家重点实验室, 上海 200240)

**摘 要:** 镁合金具有良好的生物相容性、优良的力学性能以及可完全降解的特点, 是制备血管支架的理想材料。然而在支架植入初期, 支架表面平滑肌细胞增殖速率超过内皮细胞增殖速率, 导致支架内再狭窄的发生。近年来, 在材料表面构筑微纳尺度形貌, 通过调控血管内皮细胞和平滑肌细胞行为, 实现支架表面快速内皮化成为一种新的研究思路。从基底材料、形貌特征、制备工艺、细胞种类以及实验结果等方面, 系统地总结了近年来关于材料表面微纳形貌对血管细胞行为的影响。因为目前镁合金表面微纳形貌对血管细胞行为影响的报道尚少, 从镁合金种类、形貌制备工艺、形貌特征以及形貌功能等方面详细整理了不同研究领域, 在镁合金表面制备微纳形貌的相关研究。与此同时, 分析了在镁基血管支架表面制备微纳尺度形貌用于实现支架表面快速内皮化研究所面临的挑战, 并介绍了本课题组相关研究工作进展。

**关键词:** 镁合金血管支架; 支架再内皮化; 表面微纳形貌; 血管内皮细胞; 血管平滑肌细胞

**中图分类号:** TG174.44 **文献标识码:** A **文章编号:** 1001-3660(2019)07-0332-08

**DOI:** 10.16490/j.cnki.issn.1001-3660.2019.07.038

Review on Influence of Micro-nano Scale Surface  
Topography on Vascular Cells Responses

LI Yu-tong, PEI Jia, YUAN Guang-yin

(The State Key Lab of Metal Matrix Composites, National Engineering Research Center of Light Alloy Net Forming,  
School of Materials Science and Engineering, Shanghai Jiaotong University, Shanghai 200240, China)

**ABSTRACT:** Magnesium alloys are promising materials to prepare the vascular stent due to the favorable biocompatibility, excellent mechanical properties and perfect biodegradable property. However, in-stent restenosis (ISR) still remains in the primary stage of implantation because of the excessive proliferation of vascular smooth muscle cells (SMCs) over endothelial cells (ECs). Recently, micro-nano scale surface topography construction provides a prospective strategy for rapid re-endothelialization via regulating the behavior of both ECs and SMCs. The work systematically summarized the influence of micro-nano surface topography on vascular cells from the aspects of substrate materials, topography features, preparation methods, cell types and test results. As there were few reports on the influence of micro-nano surface topography of magnesium alloys on the cell re-

收稿日期: 2019-01-15; 修订日期: 2019-02-28

Received: 2019-01-15; Revised: 2019-02-28

基金项目: 国家自然科学基金 (51701041)

Fund: Supported by National Natural Science Foundation of China (51701041)

作者简介: 李昱彤 (1993—), 男, 硕士研究生, 主要研究方向为镁合金生物材料表面改性。

Biography: LI Yu-tong (1993—), Male, Master, Research focus: surface modification of magnesium alloy biomaterials.

通讯作者: 裴佳 (1982—), 女, 博士, 副研究员, 主要研究方向为可降解仿生医用涂层及功能研究。邮箱: jpei@sjtu.edu.cn

Corresponding author: PEI Jia (1982—), Female, Doctor, Associate professor, Research focus: degradable biomimetic medical coating and functional research. E-mail: jpei@sjtu.edu.cn

sponses, relevant researches on fabrication of micro-nano topography on magnesium alloys surface in different fields were introduced in detail from type of magnesium alloy, topography fabrication process, topography characteristics, topography functions, etc. Meanwhile, the challenges of applying micro-nano scale topography to promote rapid re-endothelialization of Mg-based vascular stents were analyzed and the corresponding research progress in the research group was presented.

**KEY WORDS:** magnesium alloy vascular stent; stent re-endothelialization; micro-nano scale surface topography; vascular endothelial cells; vascular smooth muscle cells

冠心病 (Coronary Heart Disease, CHD) 是全球死亡率最高的疾病之一。支架植入疗法是目前治疗冠心病的常用方法。支架植入过程会导致血管内皮层破裂, 促进平滑肌细胞、纤维结缔组织等过度增生, 引发支架内再狭窄 (In-Stent Restenosis, ISR)。目前临床使用的支架主要是以永久性金属支架为基材的药物洗脱支架 (Drug Eluting Stent, DES)。永久性支架材料的存在, 会影响血管正常舒缩功能, 同时药物的释放不加选择地抑制了血管相关细胞的增殖<sup>[1]</sup>。因此, 一种可以在服役结束后自动“退场”, 同时又能特异性抑制平滑肌细胞增殖而不抑制甚至促进内皮细胞的增殖血管支架, 是生物材料工作者追求的理想支架模型, 可降解血管支架 (Bioresorbable vascular stent, BVS) 的出现为这种理想支架模型提供了一种思路。

BVS 按照基底材料可分为可降解聚合物支架和可降解金属 (镁、铁、锌) 支架。雅培公司 2016 年 7 月上市的可降解聚合物支架 Absorb III 的随访结果表明: 使用 BVS 患者的主要不良心血管事件相对于 DES 有所增加。因而被 FDA 提出谨慎使用的警告, 已在全球范围内停止销售, 这为可降解聚合物支架的发展蒙上了阴影。铁基材料会干扰核磁共振成像, 临近组织受到射频影响后会引发局部加热, 另外支架会受到周围磁场的影响<sup>[2]</sup>。而锌基材料还处于研发初期, 目前对锌合金在血管环境中的认识还较少。镁基材料因其较高的生物安全性、合适的力学性能<sup>[3]</sup>以及镁离子多种特殊的生理功能<sup>[4]</sup>, 成为目前最有望实现临床应用的 BVS。

镁基材料用作血管支架还需解决三个问题: 如何降低镁基材料降解速率? 如何进一步提高镁基材料生物相容性? 如何应对支架植入后带来的支架内再狭窄 (In-Stent Restenosis, ISR)? 上海交通大学材料学院袁广银教授课题组通过合金化, 开发出具有均匀降解特性和较低腐蚀速率的具有自主知识产权的 Mg-Nd-Zn-Zr 系列合金 (JDBM)<sup>[5-7]</sup>, 并在此基础上制备出血管支架产品原型。与此同时, 该课题组通过功能化涂层的方法, 显著提高了镁基材料的生物相容性<sup>[8-9]</sup>。因此, 若能在镁合金表面实现特异性抑制血管平滑肌细胞增殖, 促进血管内皮细胞增殖, 避免 ISR 发生, 即有望成为理想的支架模型。

在体内, 血管内皮层是位于具有多种物理化学特征的基底膜上的单层内皮细胞。基底膜是具有纳米

(1~100 nm)、亚微米 (100~1000 nm) 尺度, 由孔和纤维构成的复杂的网状结构<sup>[11]</sup>。目前对于血管相关细胞的研究主要集中在化学信号 (Chemical Cue) 与可溶性因子的影响, 而物理信号 (Physical Cue) 方面的研究则很少, 其中材料表面形貌是物理信号中较为重要的因素。

材料表面形貌通过接触诱导的方式影响细胞的增殖、粘附和迁移等过程, 这种诱导会因细胞类型和形貌特征尺寸的不同而有所差异。物理信号相对于化学信号而言, 仅对粘附在材料表面的细胞有影响, 无副作用。因此, 在支架表面制备微纳形貌, 为特异性促进血管内皮细胞增殖的同时抑制平滑肌细胞增殖提供了一种可能。材料表面微纳形貌对血管相关细胞的影响已有很多研究报道, 而在镁合金表面制备微纳形貌, 并研究其对血管相关细胞的影响仍鲜有报道。本文将对材料表面微纳形貌对血管相关细胞的影响以及镁合金表面微纳形貌制备方法进行综述。

## 1 材料表面微纳形貌对血管相关细胞的影响

物理信号常与化学信号耦合在一起, 没有先进的表面加工技术, 很难将众多影响因素分离开。因此, 长期以来关于基底膜的物理信号尤其是表面形貌对血管相关细胞的影响研究甚少。20 世纪 60 年代, 表面微观形貌加工最重要的一项技术——光刻技术被发明<sup>[12]</sup>。20 世纪末, 哈佛大学两个小组合作, 将光刻技术应用到细胞学研究中<sup>[13]</sup>, 在材料表面制备出不同直径的微米尺度岛状形貌, 研究结果发表在《科学》杂志中。结果表明: 岛状结构通过控制细胞形态来影响细胞的生长和凋亡。这篇文章推动了人们对材料表面形貌影响细胞行为的研究。现今很多制备材料表面形貌的技术: 光刻、微流控制、激光雕刻、飞秒激光、嵌段共聚物自组装技术、等离子刻蚀和化学刻蚀等, 被用来研究材料表面形貌和细胞之间的关系。

目前对物理形貌的研究, 按照材料表面形貌特征可以分为线性沟槽、微柱、微孔、纳米管等规则形貌, 以及用粗糙度表示的形貌。研究的基底材料包括高分子聚合物 (PDMS、PVC、PS 和 PLA 等)、陶瓷 (硅和非晶玻璃)、金属 (氧化铝、氧化钛和钴铬合金) 等。近年来报道的物理形貌对血管相关细胞的研究结果总结归纳于表 1—3。

表 1 不同类型的材料表面微纳形貌对血管相关细胞的影响 (沟槽形貌)

Tab.1 Effects of micro-nano scale topographies on surfaces of different materials on vascular cells (Grooves and ridges)

Topographies	Methods	Materials and cells	Topography features	Results
Grooves and ridges <sup>[14]</sup>	Photolithographic	PDMS Human coronary artery endothelial cells (ECs), human coronary artery smooth muscle cells (SMCs) and Human fibroblast cells (FCs)	Groove widths: 50, 100 and 200 nm Groove depths: 2, 3, 5 and 10 $\mu\text{m}$	Smaller lateral dimensions or deeper grooves induced more contact guidance. FCs responded to 50 nm groove depth; ECs and SMCs responded to 100 nm groove depth.
Grooves and ridges <sup>[15]</sup>	Photolithographic, soft lithography	NOA81 polyurethane Human umbilical vein endothelial cells (HUVECs), human dermal microvascular endothelial cells, human aortic endothelial cells, human saphenous vein endothelial cells	Groove and ridge widths: 400, 800, 1200, 1600, 2000, 4000 nm Groove depths: 300 nm	Widths > 800 nm induced cells orientation and alignment. Widths = 400 nm, inhibited the proliferation of HUVECs. Cells migrated parallel to the long axis of the ridges.
Grooves and ridges <sup>[16]</sup>	Photolithography and deep reactive-ion etching	Si wafers with $\text{TiO}_2$ coating Human umbilical vein endothelial cells (HUVECs), human umbilical artery smooth muscle cells (HUASMCs) and platelet	Groove widths: 0.5, 1, 5, 10, 20 and 50 $\mu\text{m}$ Groove depths: 3.5 $\mu\text{m}$	Groove widths with 1 $\mu\text{m}$ , enhanced HUVECs adhesion, proliferation and functionality, and reduced platelet adhesion and activation.
Grooves and ridges <sup>[18]</sup>	Photolithographic, soft lithography	PVC EA.hy926	Groove widths: 2.0 and 1.0 $\mu\text{m}$ Groove depths: 2.0 and 7.0 $\mu\text{m}$	Groove widths with 2 $\mu\text{m}$ enhanced cells adhesion significantly.
Grooves and ridges <sup>[17]</sup>	Direct laser interference patterning	CoCr alloy Human umbilical vein endothelial cells (HUVECs) and platelet	Groove and ridge widths: 3, 10, 20, 32 $\mu\text{m}$ Groove depths: 40 and 600 nm	Groove depth with 600 nm enhanced ECs elongation and migration along groove.
Grooves and ridges <sup>[28]</sup>	Photolithographic, wet etching techniques	Si human aortic endothelial cells (HAECs)	Slope-shaped groove: ridge height 25 $\mu\text{m}$ , width 15 and 40 $\mu\text{m}$ ; groove width 30~32 $\mu\text{m}$ , space 15~20 $\mu\text{m}$ . V-shaped grooves: ridge height 25 $\mu\text{m}$ , width 15 and 40 $\mu\text{m}$ , groove width 35~37 $\mu\text{m}$ , space 0 $\mu\text{m}$ .	Cells density on V-shaped groove higher than on slope-shaped. Cells alignment along groove. Groove topography inhibited cells proliferation.
Grooves and ridges <sup>[29]</sup>	Ultraviolet (UV)-assisted capillary force lithography	PET EA.hy926 endothelial cells	Ridge width: 550 nm, depth: 600 nm Groove widths: 550 nm, 1.10 $\mu\text{m}$ , and 2.75 $\mu\text{m}$	Induced cells elongation and decreased the secretion of inflammatory cytokines.
Grooves and ridges <sup>[30]</sup>	Photolithographic and plasma etching techniques	PGS Bovine aortic endothelial	Groove and ridge width: 2.5, 4.1 and 4.5 $\mu\text{m}$ Groove height: 0.45 $\mu\text{m}$	Induced cells elongation and alignment along groove.
Grooves and ridges <sup>[14]</sup>	Direct laser ablation	PU Human umbilical vein endothelial cells	Groove and ridge width: 1 and 10 $\mu\text{m}$ Groove widths: 5.5, 0.6 $\mu\text{m}$ Groove depths: 0.7, 0.4 $\mu\text{m}$	Improved cells adhesion and proliferation. Groove and ridge width = 1 $\mu\text{m}$ , enhanced cells adhesion significantly, induced cells elongation and alignment along groove.

目前公认的线性沟槽形貌对血管相关细胞的影响主要在于使细胞沿沟槽方向线性排列和生长<sup>[14-17]</sup>。部分研究表明,当沟槽宽度为 1  $\mu\text{m}$ <sup>[16]</sup>或 2  $\mu\text{m}$ <sup>[18]</sup>时,内皮细胞的粘附、增殖和生长被促进。柱状形貌会促进血管相关细胞伪足的生长<sup>[18]</sup>。多数研究表明,柱状

形貌会抑制内皮细胞和平滑肌细胞的粘附和增殖,同时抑制血小板的粘附和活性<sup>[16]</sup>。但也有研究指出,柱状形貌会促进血管相关细胞的粘附和增殖<sup>[20]</sup>。除了用光刻等技术在材料表面制备规则形貌外,一些研究者通过化学刻蚀<sup>[21]</sup>、气相沉积<sup>[22]</sup>、嫁接高分子<sup>[23]</sup>等方

表 2 不同类型的材料表面微纳形貌对血管相关细胞的影响 (微柱和微孔形貌)

Tab.2 Effects of micro-nano scale topographies on surfaces of different materials on vascular cells (pillar and well topography)

Topographies	Methods	Materials and cells	Topography features	Results
Pillar and well <sup>[20]</sup>	Direct laser ablation	PU Human umbilical vein endothelial cells	Widths: 1, 10 $\mu\text{m}$	Enhanced ECs adhesion and proliferation.
Pillars and well <sup>[19]</sup>	Photolithography and soft lithography	PDMS and PCL human fibroblast cell line (hTERT)	Pillars and pits with the same size. Dimensions: 4.2 $\mu\text{m}$ . Space: 14, 28 and 42 $\mu\text{m}$ . Height: 1.6, 6.8, 10, 14.6, 17.5 $\mu\text{m}$	More distinct protrusions were observed on 10 and 17 $\mu\text{m}$ height pillars topography.
Pillar and well <sup>[32]</sup>	Anodic aluminum oxide, nanoimprinting lithography	PS human endothelial colony-forming cells (hECFCs)	Diameter ranges: 120~200, 200~280 and 280~360 nm Center to center distance: 440 nm Height: 276.9, 268.1, 293.6 nm	Decreased area and perimeter of cells. 120/200 nm increased the number of filopodial outgrowths significantly. Nanostructural stimuli are affected by ROCK signaling
Pillar and well <sup>[16]</sup>	Photolithography and deep reactive-ion etching	Si with TiO <sub>2</sub> coating Human umbilical vein endothelial cells (HUVECs), human umbilical artery smooth muscle cells (HUASMCs) and platelet	Widths: 0.5, 1, 5, 10, 20 and 50 $\mu\text{m}$ Height: 3.5 $\mu\text{m}$	Pillars inhibited cells growth. Pillars with 1 $\mu\text{m}$ width reduced platelet adhesion and activation.

表 3 不同类型的材料表面微纳形貌对血管相关细胞的影响 (其他形貌)

Tab.3 Effects of micro-nano scale topographies on surfaces of different materials on vascular cells (other topographies)

Topographies	Methods	Materials and cells	Topography features	Results
Brush-like patterns <sup>[23]</sup>	Polymerization	PU-PEG Human umbilical vein endothelial cells	Ra: 1.53, 18.63, 20.10, 39.79 and 34.58 nm	Rougher surfaces enhanced the adhesion and growth of cells.
Micropores and microgrooved <sup>[21]</sup>	Mechanical polishing, sandpaper grinding and chemical pickling	NiTi alloy Bovine aortic endothelial cells	Ra: 16.7, 63.8, 94.4 and 519.2 nm	Rougher surfaces enhanced cell adhesion. Micropores showed much more endothelialization than microgrooved surface after a 3 days culture
Conical spikes <sup>[33]</sup>	Femtosecond (fs) laser	Si wafers NIH-3T3	Roughness ratio (conical spokes' density): 2.6, 3.3, 6.0 and 6.9	Best adhesion of cells were observed on small roughness ratios surface.
Nanowires <sup>[22]</sup>	Chemical vapour deposition	Al <sub>2</sub> O <sub>3</sub> Human umbilical vein endothelial cells (HUV-EC), human umbilical vein smooth muscle cells (HUVSMC)	Low density nanowires, Ra=21, 29 nm High density nanowires, Ra=187, 272 nm	HUVSMCs appear to be more sensitive to changes in topography than HUVECs
Random patterns <sup>[24]</sup>	Ion-beam deposition process	Pure titanium deposited on glass coverslips Rat aortic endothelial cells	RMS values: 0.5, 1 and 14 nm Lateral: 0, 30~40 and above 100 nm Vertical: 0, 2~6 and 20~40 nm	Maximum roughness surface had the largest contact area with cells, the smallest contact angle, the lowest surface energy, and the cell density was 4 times than negative control.
Vascular smooth muscle cell biomimetic surface patterns (microgrooves) <sup>[34]</sup>	Femtosecond laser	316L cardiovascular stents Implanted into iliac artery of rabbits	Microgroove periodicity: 2 $\mu\text{m}$ , height: 100 nm	Enhanced the adhesion, proliferation and migration of cells. The patterned surfaces can significantly enhance re-endothelialization.
Islands <sup>[31]</sup>	Polymer demixing	PS-PBrS Human endothelial cell type, HGTFN	Height: 13, 35 and 95 nm	Cell spread better on island topography than flat surface. The height of 13 nm enhanced ECs spread significantly.

法,在材料表面构筑粗糙形貌来调控血管相关细胞的增殖。这类形貌通过改变表面粗糙度来影响细胞与材料间的接触面积,进而调控细胞应力纤维和伪足的形成,最终影响细胞粘附和功能表达。还有研究表明,表面形貌是通过影响表面能、浸润性以及细胞与材料之间的应力分布等因素来调控细胞<sup>[24]</sup>。

血管内皮细胞需要特异性的粘附基底、信号和骨架动力学,来调控其在血管再生过程中的运动,影响这一个复杂细胞迁移过程的重要因素是细胞肌动蛋白骨架对肌球蛋白的调节作用<sup>[25]</sup>。肌球蛋白的位置和功能主要受 RhoA (一种小的 GTP 酶) 的调控<sup>[26]</sup>。收缩性和 RhoA 进一步影响细胞多种突起的形成,比如:丝状伪足、板状伪足和膜泡等,三种突起之间的转换对于内皮细胞在复杂三维环境中的迁移至关重要<sup>[27]</sup>。材料表面形貌会影响细胞丝状伪足的形成,因此表面微纳形貌很有可能就是实现支架表面附近快速内皮化的关键。综上,通过调控材料表面微纳形貌,选择性地促进快速内皮化,同时抑制平滑肌细胞和纤维结缔组织的快速增生,为解决 ISR 提供了一种可行的改进策略。

尽管材料形貌与细胞之间的相互作用已经研究了二十多年,但是,因为使用材料不统一、制备方法多样、形貌尺度不一以及选择的细胞不尽相同等问题,使得目前仅有线性沟槽形貌可定向诱导细胞伸长、迁移、排列这一共识,并且沟槽尺寸对细胞特异性影响也说法不一。因此,需要统一且系统的方式来原因材料表面形貌对细胞的影响。另外,材料表面形貌对血管相关细胞的研究仅停留在不可降解材料,对于可降解材料(如聚乳酸、镁合金等)鲜有报道。

## 2 镁及镁合金表面微纳形貌的构筑

材料表面物理形貌的调控为支架表面促进快速内皮化提供了一种可行的改进策略。镁基血管支架作为新一代可降解血管支架的研究代表,研究镁合金表面物理形貌对血管相关细胞的影响尤为重要。

近年来关于镁及镁合金材料表面微纳形貌制备的报道如表 4 所示。研究主要集中在纯镁、AZ91、AZ31、WE43 等商用材料,以及自主研发的 JDBM 镁合金、镁铝合金、镁钇合金和镁锂合金。在镁合金表

表 4 镁合金表面微纳形貌相关研究  
Tab.4 Research of micro-nano topography of magnesium alloy

Materials	Methods	Topography feature	Topography function
Pure Mg <sup>[40]</sup>	Electrodeposition method	Flake-like topography	Improved corrosion resistance and biocompatibility
Pure Mg <sup>[42]</sup>	High-flux C ion irradiation	Regular wave (comb) structure	Study the effects of high intensity pulsed beam irradiation on the surface of magnesium alloy
Pure Mg and Mg-Y alloy <sup>[46]</sup>	Transonic particle acceleration process mesenchymal stemcells	Homogeneous CaP coatings particulate surface	Improved cells adhesion
Mg alloy AZ91D <sup>[41]</sup>	Laser surface melting treatments	Corrugated topography	Remove material surface defects and improve corrosion resistance
Mg alloy AZ91D <sup>[43]</sup>	Electro-deposition process	Cauliflower-like cluster binary micro-nano structural	Super-hydrophobic surface, improve corrosion resistance
Mg alloy AZ91 <sup>[36]</sup>	Micro-arc oxidation, fluoridation and electrophoretic deposition method	Flake-like topography	Improve corrosion resistance
Mg alloy AZ31 <sup>[35]</sup>	Micro-arc oxidation	Micro-pore structure	Super-hydrophobic surface, improve corrosion resistance
Mg alloy AZ31 <sup>[44]</sup>	Chemical etching, deposition of biocompatible siloxane coating	Hierarchical surface structure, microscale spherical features and nanoscale rod-like structures, mimic the surface structure of the lotus leaf	Super-hydrophobic surface
Mg alloy AZ31 <sup>[47]</sup>	Microwave aqueous approach MC3T3-E1	Micron/submicron scale resorption lacunae and nano-scale sharp-tipped collagen fibrils	Enhanced osteogenic differentiation capacity and corrosion resistance.
Mg alloy AZ31B <sup>[38]</sup>	Hydrofluoric acid and in situ hydrothermal synthesis methods	Dense micron-sized packed granular morphology	Super-hydrophilicity and enhanced corrosion resistance
Mg alloy WE43 and EW62 <sup>[39]</sup>	Ambient temperature blast coating technique	$Ra=1.6\ \mu\text{m}$	Enhanced corrosion resistance
Mg alloy WE43 <sup>[37]</sup>	Electrophoretic deposition	Stacked granular morphology	Enhanced bioactivity and hardness

续表

Materials	Methods	Topography feature	Topography function
Mg alloy JDBM <sup>[8]</sup>	Fluoridation HUVECs	Flake-like topography	Enchanted corrosion resistance and biocompatibility
Mg alloy JDBM <sup>[48]</sup>	Fluoridation, Calcium phosphate deposition MC3T3-E1	Flake-like topography	Enchanted corrosion resistance and biocompatibility
Mg alloy ZK60 <sup>[49]</sup>	One-pot hydrothermal process Bone marrow stromal cell	Cluster crystal morphology	Control the degradation and enhance osteoinduction activity and antibacterial properties
5083Al-Mg <sup>[50]</sup>	Electrochemical etching and boiling water treatment methods	Dense nanoscale needle-like topography	Superhydrophobic
Ultrafine-Grained LZ91 Mg-Li alloy <sup>[45]</sup>	Micro-embossing	Micro-array channels. Widths: 50, 100, 150, 200 μm	For micro-electro-mechanical system (MEMS) components

面制备微纳形貌的方法包括：微弧氧化<sup>[35-36]</sup>、电泳沉积<sup>[37]</sup>、水热合成<sup>[38]</sup>、室温喷涂<sup>[38]</sup>、电沉积<sup>[40]</sup>、激光烧灼<sup>[41]</sup>、超声速离子沉积<sup>[42]</sup>、电镀法<sup>[43]</sup>、化学沉积<sup>[44]</sup>、化学刻蚀<sup>[44]</sup>以及高温压印技术<sup>[44]</sup>等。目前仅高温压印技术，在超细晶粒 LZ91 镁合金表面得到可控的微米尺度线性沟槽形貌<sup>[45]</sup>，而其他方法得到的形貌大多为尺寸难以精确控制的均匀形貌，比如：团簇的颗粒、层片状、立柱桩和微孔等形貌。镁合金表面微纳形貌的制备，主要用于制备超疏水或超亲水层，进而提高材料的耐蚀性能。

镁合金表面微纳形貌对细胞的影响仅有几篇文献报道。这些研究均将化学信号与物理信号耦合在一起进行研究，仅停留在定性地认为表面形貌影响了细胞应答，没有系统地研究不同表面形貌对细胞应答的影响，更不必说对血管相关细胞的研究。因此，镁合金表面微纳形貌对血管相关细胞的影响尚没有系统的研究，这还需要科研工作者们不懈的努力。

3 微纳形貌促进镁基血管支架表面快速内皮化的研究与挑战

上海交通大学袁广银教授课题组通过化学刻蚀的方式，在 JDBM 镁合金表面制备出粗糙度  $Sa$  为 0.2、0.5、0.8、1.2、1.8 μm 且均匀的山脊和山谷交替表面形貌，并在粗糙形貌表面制备氟化镁和聚多巴胺复合涂层，来提高样品的耐蚀性能和生物相容性。样品表面形貌扫描电镜图如图 1 所示，刻蚀出的样品表面形貌与报道中的基底膜微纳尺度复合形貌类似<sup>[11]</sup>。

在此基础上，研究了镁降解微环境及亚微米/微米表面形貌共同作用对血管内皮细胞及平滑肌细胞行为的影响规律，并优选出具有血管内皮细胞/平滑肌细胞特异性的表面粗糙度形貌参数范围。

图 2 为血管内皮细胞与平滑肌细胞密度随粗糙度  $Sa$  的变化规律，以商用细胞培养板为阴性对照。 $Sa$  为 1.2 μm 和 1.8 μm 的样品表面，内皮细胞密度显

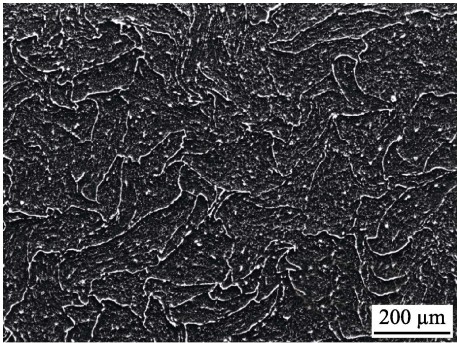


图 1 微米尺度粗糙度 JDBM 样品表面扫描电镜图  
Fig.1 SEM images of JDBM samples with micron roughness

著高于其他组样品 ( $P<0.001$ )； $Sa=1.8\text{ }\mu\text{m}$  时，样品表面细胞密度超过阴性对照组细胞密度。与此同时，不同粗糙度样品表面，平滑肌细胞密度无明显差异，均显著低于阴性对照组 ( $P<0.001$ )。因此，可认为  $Sa=1.8\text{ }\mu\text{m}$  且具有聚多巴胺和氟化镁复合涂层的 JDBM 镁合金，可显著促进血管内皮细胞的生长同时抑制平滑肌细胞的生长，这为血管支架表面实现快速内皮化提供了一种可行的策略。

本研究利用 JDBM 镁合金的腐蚀特性，用柠檬酸刻蚀，在 JDBM 金属圆片表面制备粗糙形貌。而如何将粗糙形貌制备到镁合金血管支架表面，还需要进一步探究。目前，制备镁合金血管支架的方法主要为激光雕刻镁合金毛细管材，可以选择在激光雕刻之前对管材进行刻蚀，或者在激光雕刻后对支架直接进行刻蚀。化学刻蚀可以不受样品表面起伏的影响而获得较均匀的刻蚀形貌，有望在镁合金血管支架表面得到理想的粗糙形貌，实现对血管相关细胞应答的调控。

镁合金表面微纳形貌对血管相关细胞影响的研究意义重大，尽管本课题组已获得一些研究成果，但仍有很多挑战需要克服。首先，之前的报道大多数集中在用光刻等技术在高分子或硅片表面制备微纳形貌，研究形貌对细胞行为的影响，而如何将光刻等先进技术应用在镁合金等金属材料表面，仍需进一步研究。另外，血管支架需要在内外表面都制备均匀的形



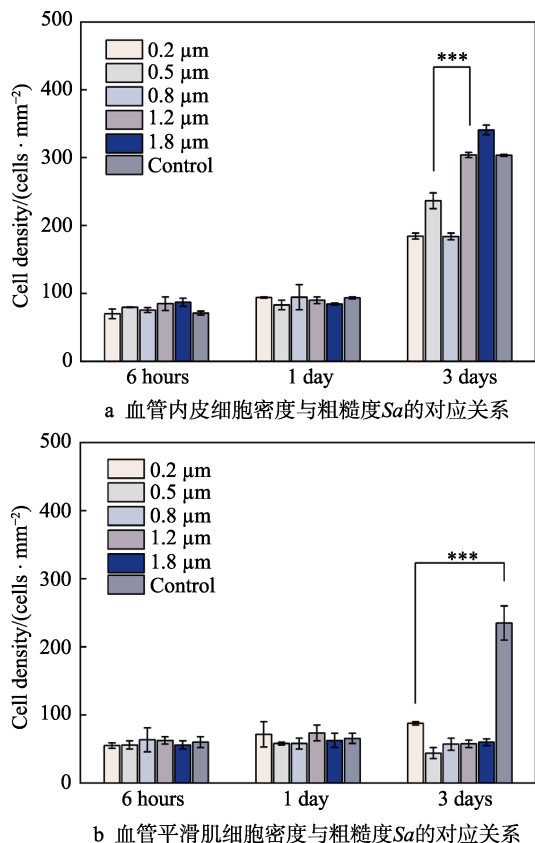


图2 细胞密度随亚微米/微米粗糙度变化规律

Fig.2 Change laws of cell density along with submicron-micron roughness

(a) Interaction between endothelial cell density and roughness Sa; (b) Interaction between smooth muscle cell density and roughness Sa

貌,这也为光刻技术的应用增加了难度。其次,现有的镁合金表面加工工艺,仅 Qian Su 等人<sup>[45]</sup>在超细晶粒 LZ91 镁锂合金表面,通过高温压印技术制备出微米尺寸沟槽形貌,然而这种方法使用的超细晶粒合金的力学性能、生物相容性以及耐腐蚀性能是否满足生物材料的要求,仍需要进一步研究。另外,该工艺是否可以应用到现有的镁合金生物材料表面也需要进一步探索。不同于传统的不可降解基底材料,镁合金作为可降解生物材料,随着细胞培养的进程会不断降解。因此,在材料表面完成内皮化之前,动态变化的表面形貌如何实现对血管相关细胞的持续调控,是一个需要面临的挑战。最后,镁合金生物材料对细胞的影响耦合了镁离子、涂层性质以及材料表面微纳形貌等,如何巧妙地设计实验,将物理信号对血管相关细胞的影响剥离出来,也是一个需要考虑的问题。

## 4 结语

当 FDA 对可降解聚合物血管支架 Absorb III 提出谨慎使用的警告时,人们把对可降解支架的希望更多地寄托于镁合金血管支架上。先进的合金化工艺和精细的表面功能化涂层修饰,已经为镁合金血管支架

提供了足够的力学性能、耐腐蚀性能和生物相容性。材料表面微纳形貌可以选择性地影响细胞应答。镁合金血管支架与材料表面微纳形貌相结合,在植入初期促进支架表面快速内皮化的进程,支架服役结束后完全降解。这为理想的血管支架模型提供了可行的方案。这需要科研工作者为之付出更多的努力,才有可能为饱受冠心病折磨的病人带来希望。

## 参考文献:

- [1] RICCARDO G, MARCO L, EDOARDO V, et al. Safety and efficacy of first-generation and second-generation drug-eluting stents in the setting of acute coronary syndromes[J]. Journal of cardiovascular medicine, 2014, 15(7): 532-542.
- [2] LIN W J, ZHANG D Y, ZHANG G, et al. Design and characterization of a novel biocorrosible iron-based drug-eluting coronary scaffold[J]. Materials & design, 2016, 91: 72-79.
- [3] ZENG R C, DIETZEL W, FRANK W, et al. Progress and challenge for magnesium alloys as biomaterials[J]. Advanced engineering materials. 2008, 10(8): 3-14.
- [4] MA J, ZHAO N, ZHU D. Biphasic responses of human vascular smooth muscle cells to magnesium ion[J]. J biomed mater res part A, 2016, 104: 347-356.
- [5] MAO L, YUAN G Y, NIU J L, et al. In vitro degradation behavior and biocompatibility of Mg-Nd-Zn-Zr alloy by hydrofluoric acid treatment[J]. Materials science and engineering C, 2013, 33: 242-250.
- [6] MAO L, YUAN G Y, WANG S, et al. A novel biodegradable Mg-Nd-Zn-Zr alloy with uniform corrosion behavior in artificial plasma[J]. Materials letters, 2012, 88: 1-4.
- [7] CHEN C, TAN J, WU W, et al. Modeling and experimental studies of coating delamination of biodegradable magnesium alloy cardiovascular stents[J]. ACS biomaterials science & engineering, 2018, 4(11): 3864-3873.
- [8] MAO L, SHEN L, CHEN J, et al. Enhanced bioactivity of Mg-Nd-Zn-Zr alloy achieved with nanoscale MgF<sub>2</sub> surface for vascular stent application[J]. ACS applied materials & interfaces, 2015, 7(9): 5320-5330.
- [9] MAO L, SHEN L, NIU J L, et al. Nanophase biodegradation enhances the durability and biocompatibility of magnesium alloys for the next-generation vascular stents[J]. Nanoscale, 2013, 5(20): 9517-9522.
- [10] ZHANG J, LI H, WANG W, et al. The degradation and transport mechanism of a Mg-Nd-Zn-Zr stent in rabbit common carotid artery: A 20-month study[J]. Acta biomaterialia, 2018, 69: 372-384.
- [11] LILIENSIEK S J, NEALEY P, MURPHY C J. Characterization of endothelial basement membrane nanotopography in rhesus macaque as a guide for vessel tissue en-

- gineering[J]. Tissue engineering: part A, 2008, 15: 19.
- [12] GLENDINNING W B, MARSHALL S, MARK A, et al. Projection photolithography for use in the of microcircuits[J]. Ieee tranctions on component parts, 1964, 9: 19-26.
- [13] CHEN C S, MRKSICH M, HUANG S, et al. Geometric control of cell life and death[J]. Science, 1997, 276: 1425-1428.
- [14] BIELA S A, SU Y, SPATZ J P, et al. Different sensitivity of human endothelial cells, smooth muscle cells and fibroblasts to topography in the nano-micro range[J]. Acta biomaterialia, 2009, 5(7): 2460-2466.
- [15] LILIENSIEK S J, WOOD J A, YONG J, et al. Modulation of human vascular endothelial cell behaviors by nanotopographic cues[J]. Biomaterials, 2010, 31(20): 5418-5426.
- [16] DING Y, YANG Z, BI C W C, et al. Directing vascular cell selectivity and hemocompatibility on patterned platforms featuring variable topographic geometry and size[J]. ACS applied materials & interfaces, 2014, 6(15): 12062-12070.
- [17] SCHIEBER R, LASSERRE F, HANS M, et al. Direct laser interference patterning of CoCr alloy surfaces to control endothelial cell and platelet response for cardiovascular applications[J]. Advanced healthcare materials, 2017, 6(19): 1700327.
- [18] CUTIONGCO M F A, GOH S H, AID-LAUNAS R, et al. Planar and tubular patterning of micro and nanotopographies on poly(vinyl alcohol)hydrogel for improved endothelial cell responses[J]. Biomaterials, 2016, 84: 184-195.
- [19] CORTESE B, RIEHLE M O, AMONE S D, et al. Influence of variable substrate geometry on wettability and cellular responses[J]. Journal of colloid and interface science, 2013, 394: 582-589.
- [20] CORTELLA L, CESTARI I A, GUENTHER D, et al. Endothelial cell responses to castor oil-based polyurethane substrates functionalized by direct laser ablation[J]. Biomedical materials, 2017, 12: 65010.
- [21] SHEN Y, WANG G, CHEN L, et al. Investigation of surface endothelialization on biomedical nitinol (NiTi) alloy: Effects of surface micropatterning combined with plasma nanocoatings[J]. Acta biomaterialia, 2009, 5(9): 3593-3604.
- [22] AKTAS C, DÖRRSCHUCK E, SCHUH C, et al. Micro- and nanostructured Al<sub>2</sub>O<sub>3</sub> surfaces for controlled vascular endothelial and smooth muscle cell adhesion and proliferation[J]. Materials science and engineering: C, 2012, 32(5): 1017-1024.
- [23] CHUNG T, LIU D, WANG S, et al. Enhancement of the growth of human endothelial cells by surface roughness at nanometer scale[J]. Biomaterials, 2003, 24(25): 4655-4661.
- [24] KHANG D, LU J, YAO C, et al. The role of nanometer and sub-micron surface features on vascular and bone cell adhesion on titanium[J]. Biomaterials, 2008, 29(8): 970-983.
- [25] LAMALICE L, LE B F, HUOT J. Endothelial cell migration during angiogenesis[J]. Circulation research, 2007, 100(6): 782-794.
- [26] SIT S T, MANSER E. Rho GTPases and their role in organizing the actin cytoskeleton[J]. Journal of cell science, 2011, 124(5): 679-683.
- [27] FRIEDL P. Prespecification and plasticity: Shifting mechanisms of cell migration[J]. Curr opin cell biol, 2004, 16(1): 14-23.
- [28] SARA Fernández-Castillejo, PILAR Formentín, ÚRSULA Catalán, et al. Silicon microgrooves for contact guidance of human aortic endothelial cells full research paper open access[J]. Beilstein J nanotechnol, 2017, 8(8): 675-681.
- [29] GONG X, YAO J, HE H, et al. Combination of flow and micropattern alignment affecting flow-resistant endothelial cell adhesion[J]. Journal of the mechanical behavior of biomedical materials, 2017, 74: 11-20.
- [30] BETTINGER C J, ORRICK B, MISRA A, et al. Micro-fabrication of poly(glycerol-sebacate) for contact guidance applications[J]. Biomaterials, 2006, 27(12): 2558-2565.
- [31] DALBY M J, RIEHLE M O, JOHNSTONE H, et al. In vitro reaction of endothelial cells to polymer demixed nanotopography[J]. Biomaterials, 2002, 23(14): 2945-2954.
- [32] CUI L, JOO H J, KIM D H, et al. Manipulation of the response of human endothelial colony-forming cells by focal adhesion assembly using gradient nanopattern plates[J]. Acta biomaterialia, 2018, 65: 272-282.
- [33] RANELLA A, BARBEROGLU M, BAKOGIANNI S, et al. Tuning cell adhesion by controlling the roughness and wettability of 3D micro/nano silicon structures[J]. Acta biomaterialia, 2010, 6(7): 2711-2720.
- [34] LIANG C, HU Y, WANG H, et al. Biomimetic cardiovascular stents for in vivo re-endothelialization[J]. Biomaterials, 2016, 103: 170-182.
- [35] CUI X, LIN X, LIU C, et al. Fabrication and corrosion resistance of a hydrophobic micro-arc oxidation coating on AZ31 Mg alloy[J]. Corrosion science, 2015, 90: 402-412.
- [36] ROJAE R, FATHI M, RAEISSI K. Electrophoretic deposition of nanostructured hydroxyapatite coating on AZ91 magnesium alloy implants with different surface treatments[J]. Applied surface science, 2013, 285: 664-673.
- [37] HEISE S, WIRTH T, HÖHLINGER M, et al. Electrophoretic deposition of chitosan/bioactive glass/silica coatings on stainless steel and WE43 Mg alloy substrates[J]. Surface and coatings technology, 2018, 344: 553-563.
- [38] LIU W, YAN Z, MA X, et al. Mg-MOF-74/MgF<sub>2</sub> composite coating for improving the properties of magnesium alloy implants: hydrophilicity and corrosion resistance[J]. Materials, 2018, 11(3): 396.



- structured calcium silicate coatings with enhanced stability, bioactivity and osteogenic and angiogenic activity[J]. *Colloids & surfaces B: Biointerfaces*, 2015, 126: 358-366.
- [9] LIU X, DING C. Plasma sprayed wollastonite/TiO<sub>2</sub> composite coatings on titanium alloys[J]. *Biomaterials*, 2002, 23(20): 4065-4077.
- [10] LIU X Y. Study on plasma sprayed bioactive wollastonite coatings[J]. *Journal of the Graduate School of the Chinese Academy of Science*, 2005, 4(22): 519-523.
- [11] QU H, WEI M. The effect of fluoride contents in fluoridated hydroxyapatite on osteoblast behavior[J]. *Acta biomaterialia*, 2006, 2(1): 113-119.
- [12] SHI L, BAI Y, SU J, et al. Graphene oxide/fluorhydroxyapatite composites with enhanced chemical stability, mechanical, and biological properties for dental applications[J]. *International journal of applied ceramic technology*, 2017, 14: 1088-1100.
- [13] SHI L, BAI Y, BAI Y L, et al. Fabrication and characterization of carbon nanotubes/fluorhydroxyapatite composites[J]. *Journal of nanoscience & nanotechnology*, 2018, 18(6): 4040-4046.
- [14] VAHABZADEH S, ROY M, BANDYOPADHYAY A, et al. Phase stability and biological property evaluation of plasma sprayed hydroxyapatite coatings for orthopedic and dental applications[J]. *Acta biomaterialia*, 2015, 17: 47-55.
- [15] LIU G, GENG X, PANG H, et al. Deposition of nanostructured fluorine-doped hydroxyapatite coating from aqueous dispersion by suspension plasma spray[J]. *Journal of the American Ceramic Society*, 2016, 99(9): 2899-2904.
- [16] XU H, GENG X, LIU G, et al. Deposition, nanostructure and phase composition of suspension plasma-sprayed hydroxyapatite coatings[J]. *Ceramics international*, 2016, 42(7): 8684-8690.
- [17] RAMPON R, MARCHAND O, FILIATRE C, et al. Influence of suspension characteristics on coatings microstructure obtained by suspension plasma spraying[J]. *Surface & coatings technology*, 2008, 202(18): 4337-4342.
- [18] PAWLOWSKI L. Suspension and solution thermal spray coatings[J]. *Surface and coatings technology*, 2009, 203(19): 2807-2829.
- [19] 孟晓明, 叶卫平, 程旭东, 等. 悬浮液等离子喷涂制备的热障涂层微观结构和性能[J]. *材料科学与工艺*, 2013, 21(3): 143-148.
- MENG Xiao-ming, YE Wei-ping, CHENG Xu-dong, et al. Microstructure and performance of TBCs produced by suspension plasma spraying[J]. *Materials science & technology*, 2013, 21(3): 143-148.
- [20] XUE W, LIU X, ZHENG X, et al. Dissolution and mineralization of plasma-sprayed wollastonite coatings with different crystallinity[J]. *Surface & Coatings Technology*, 2005, 200(7): 2420-2427.

(上接第 339 页)

- [39] DUNNE C F, LEVY G K, HAKIMI O, et al. Corrosion behaviour of biodegradable magnesium alloys with hydroxyapatite coatings[J]. *Surface and coatings technology*, 2016, 289: 37-44.
- [40] ASSADIAN M, JAFARI H, GHAFARI SHAHRI S M, et al. Topography, wetting, and corrosion responses of electrodeposited hydroxyapatite and fluoridated hydroxyapatite on magnesium[J]. *Bio-medical materials and engineering*, 2016, 27(2-3): 287-303.
- [41] TALTAUVULL C, TORRES B, LOPEZ A J, et al. Corrosion behaviour of laser surface melted magnesium alloy AZ91D[J]. *Materials & design*, 2014, 57: 40-50.
- [42] POTYOMKIN G V, LIGACHEV A E, ZHIDKOV M V, et al. The change in the surface topography of magnesium under high-flux C ion irradiation[J]. *Journal of physics: Conference series*, 2015, 652: 12005.
- [43] LIU Y, YIN X, ZHANG J, et al. A electro-deposition process for fabrication of biomimetic super-hydrophobic surface and its corrosion resistance on magnesium alloy[J]. *Electrochimica acta*, 2014, 125: 395-403.
- [44] GRAY-MUNRO J, CAMPBELL J. Mimicking the hierarchical surface topography and superhydrophobicity of the lotus leaf on magnesium alloy AZ31[J]. *Materials letters*, 2017, 189: 271-274.
- [45] SU Q, XU J, WANG C, et al. The fabrication of micro-array channels with the ultrafine-grained LZ91 Mg-Li alloy by micro-embossing[J]. *Micromachines*, 2018, 9(2): 55.
- [46] ISKANDAR M E, ASLANI A, TIAN Q, et al. Nanostructured calcium phosphate coatings on magnesium alloys: Characterization and cytocompatibility with mesenchymal stem cells[J]. *Journal of materials science: Materials in medicine*, 2015, 26(5): 189.
- [47] SHEN S, CAI S, BAO X, et al. Biomimetic fluoridated hydroxyapatite coating with micron/nano-topography on magnesium alloy for orthopaedic application[J]. *Chemical engineering journal*, 2018, 339: 7-13.
- [48] ZHANG L, PEI J, WANG H, et al. Facile preparation of poly(lactic acid)/brushite bilayer coating on biodegradable magnesium alloys with multiple functionalities for orthopedic application[J]. *ACS applied materials & interfaces*, 2017, 9(11): 9437-9448.
- [49] YANG G, YANG H, SHI L, et al. Enhancing corrosion resistance, osteoinduction, and antibacterial properties by Zn/Sr additional surface modification of magnesium alloy[J]. *ACS biomaterials science & engineering*, 2018, 4(12): 4289-4298.
- [50] MA N, CHEN Y, ZHAO S, et al. Preparation of superhydrophobic and superoleophobic Al-Mg alloy surface via simple, environmentally friendly method[J]. *Journal of materials research*, 2018, 33(22): 3818-3826.